Modeling of Atomic Processes of Multiple Charged Ions in Plasmas and Its Application to the Study of EUV Light Sources*)

Akira SASAKI, Katsunobu NISHIHARA[1)], Atsushi SUNAHARA[2)], Hiroyuki FURUKAWA[2)], Takeshi NISHIKAWA[3)] and Fumihiro KOIKE[4)]

Quantum Beam Science Directorate, Japan Atomic Energy Agency, Kizugawa 619-0215, Japan
[1)]*Institute of Laser Engineering, Osaka University, Suita 565-0871, Japan*
[2)]*Institute for Laser Technology, Osaka 550-0004, Japan*
[3)]*Department of Electrical and Electronic Engineering, Okayama University, Okayama 700-8530, Japan*
[4)]*Physics Laboratory, School of Medicine, Kitasato University, Sagamihara 228-8555, Japan*

(Received 21 December 2010 / Accepted 21 March 2011)

Atomic processes of multiple-charged ions of high-Z elements from tin to dysprosium are investigated for their application to light sources for extreme-ultra-violet (EUV) lithography. Modeling of these ions in plasmas, including tungsten, which is being considered for use as a divertor and wall material in the fusion devices, is discussed. Atomic spectra become very complex in the case of low-charged ions below Pd-like ions, which calls for a new atomic code for calculating the energy levels and rate coefficients of collisional and radiative processes. The collisional radiative model is validated through code comparison workshop activities. An alternative method for investigating the formation of the non-uniform structure of the plasmas is also presented.

Keywords: atomic process, radiative transfer, EUV, lithography

DOI: 10.1585/pfr.6.2401145

1. Introduction

Sn and Xe plasmas pumped by laser irradiation or discharge have been attracted attention for their application to the semiconductor lithography. Using Sn plasmas, more than 100 W of EUV emission at the wavelength of 13.5 nm has been achieved, and semiconductor devices with a critical dimension of 22 nm have been fabricated [1, 2].

Recently, extension of the plasma light sources to shorter wavelengths is being considered for next-generation EUV lithography [3, 4], using multilayer optics with a reflectivity of 40% at $\lambda = 6.5$ nm.

We herein present results of analysis of atomic processes of Sn to W plasmas. We also describe development of a collisional radiative (CR) model of these atomic elements. Taking the detailed spectral structure of emission lines into account, we calculate the emission spectrum as well as the spectral efficiency of the plasmas [5]. Furthermore, the coefficients of radiative transfer, namely spectral emissivity and opacity, are calculated for the radiation hydrodynamics simulation in order to determine the optimum condition of the light source. This optimum condition is determined to obtain high output power and efficiency with respect to pumping conditions such as the target material, laser wavelength, intensity, and pulse duration.

The CR model is applicable to the analysis of radiation loss from tungsten in the fusion plasmas. However, the atomic number of tungsten is large. Thus, the emission spectrum from low-charged ions of tungsten, which has a significant abundance in the divetor plasmas, is extremely complex. Such a complex spectrum is difficult to calculate [6]. Therefore, we discuss a possible improvement in the model in terms of calculation of atomic physics and atomic processes. In addition, we present an alternative method based on non-equilibrium statistical mechanics to understand the occurrence of plasma non-uniformity, which is caused by the effects of atomic processes and radiative transfer.

2. Atomic Model

We calculate atomic energy levels and radiative rate coefficients of high-Z ions using the HULLAC code [7]. Figure 1 shows the energy level diagram of two Nb-like ions, with a ground configuration of $4p^6 4d^5$. Efficient emission in the EUV wavelength region arises from $4d - 4f + 4p - 4d$ transition arrays from Pd-like to Br-like ions with a ground configuration of $4d^n$. Figure 2 shows gA, which is a product of the radiative decay rate and the statistical weight of the $4d - 4f + 4p - 4d$ transition array of Nb-like Sn, Xe, Nd, and Gd ions. It can be seen that the spectral profiles of those ions are similar, except for a shift in peak toward shorter wavelength with an increase in the atomic number. Emission occurs from resonance lines to the ground state and also through satellite lines between excited states.

author's e-mail: a_sasaki@osa.att.ne.jp

*) This article is based on the presentation at the 20th International Toki Conference (ITC20).

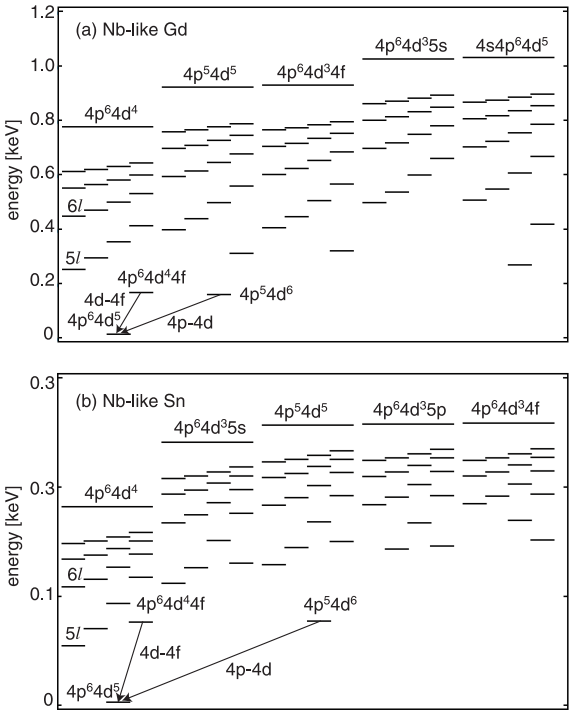

Fig. 1 Energy level diagram of Nb-like Gd (a) and Sn (b) based on the energy levels calculated using the HULLAC code [7].

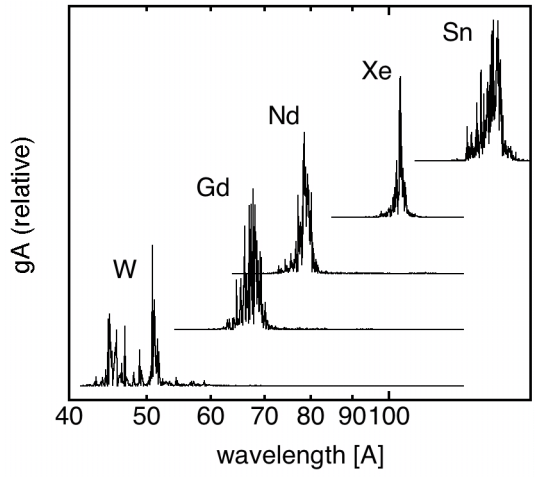

Fig. 2 gA values of $4d-4f+4p-4d$ transition array of Sn, Xe, Nd, Gd, and W.

We calculate the level population by calculating the CR model using the configuration model. High-Z ions usually have a large number of energetically closely spaced fine structure levels for each configuration. However, in high density plasmas, the population of fine structure levels can be assumed to be in thermal equilibrium, thus we calculate the population for each configuration using averaged energy levels and rate coefficients. Optically thin condition is also assumed. The set of energy levels to be included in the CR model is chosen after an iterative calculation of level population by increasing the number of groups of levels until convergence is achieved. A typical calculation is performed using 5 groups of configurations such as $4p^64d^4nl$, $4p^54d^{10}nl$, and $4p^64d^3(4f|5s|5p)nl$ configurations, as shown in Fig. 1. After the level population is determined, the spectral emissivity and opacity are calculated using the detailed profile of the emission lines calculated by the HULLAC code by taking the effect of configuration interaction (CI) into account. From the calculated spectral emissivity we determine the spectral efficiency, namely the ratio of emission from the central wavelength in the 2% bandwidth range to the total emission.

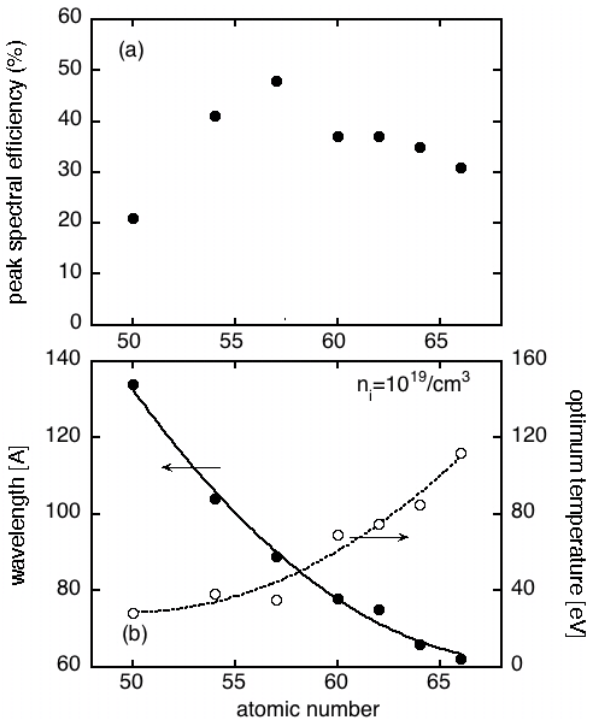

Fig. 3 Atomic number dependence of the peak spectral efficiency (a) and wavelength of the emission line and optimum temperature (b) of Sn to Dy plasmas, at an ion density of $n_i = 10^{19}/\mathrm{cm}^3$.

Figure 3 summarizes the calculated results. We repeat calculations of the spectral efficiency over the possible range of electron temperatures and ion densities in laser and discharge-pumped plasmas. It is shown that the maximum spectral efficiency is within the range of 30-40% for elements with atomic numbers from 54 to 66. We determine the optimum temperature for which the maximum spectral efficiency is obtained for a typical ion density of 10^{19} cm^{-3}, which increases from 40 to 100 eV as the wavelength decreases from 13.5 nm for Sn to 6.2 nm for Dy.

We have also estimated the conversion efficiency (CE) from the pumping laser intensity to the output EUV power using the power balance model [9], which shows that a CE similar to that of Sn of 8% can be obtained for Gd and Tb. On the other hand, it is found that the radiation power loss increases as T_e^4. This trend arises from the fact that at

each electron temperature of the plasma, these ions have a large opacity at the photon energy $\approx 2.82 k_B T_e$. As the radiation power loss increases as Planck's law; accordingly, the pumping laser intensity should be increased tenfold [8].

Results of calculation of the atomic processes of Sn to Dy ions are useful in the development of the EUV sources. However, detailed comparisons between experimental and calculated results for the Sn plasma suggest that an improvement of theoretical models is required for further investigations of atomic processes and radiative properties of high-Z plasmas.

Figure 4 shows a comparison between calculated and experimental [10] emission spectra of Nb-like Sn. The wavelength of the calculated spectrum is shorter than that of the experimental spectrum. Averaged width of the transition array seems similar, however, the detailed structure is different. Moreover, the effect of emission from excited states should be taken into account in the observed spectrum. Note that in the case of heavier ions such as tungsten ($Z = 74$), for which low charged ions have $4f$ open-shell structure, the emission spectrum becomes is more complex, which can not be calculated using any of the existing atomic codes.

Identification of the emission lines and analysis of the plasma condition can be done by obtaining an agreement between experimental and calculated spectrum, which is obtained by coupled atomic physics and CR-model calculations. In the case of complex high-Z ions, a set of configurations to calculate atomic wavelength taking the effect of CI into account should be decided. Another set of configurations should be chosen to include emission from the excited states. Furthermore, density and temperature also should be optimized to obtain agreement of the spectrum, because in experiments exact density and temperature are not usually given. Thus, optimization should be carried out within a wide parameter space, for which a system based on machine learning algorithm should be useful.

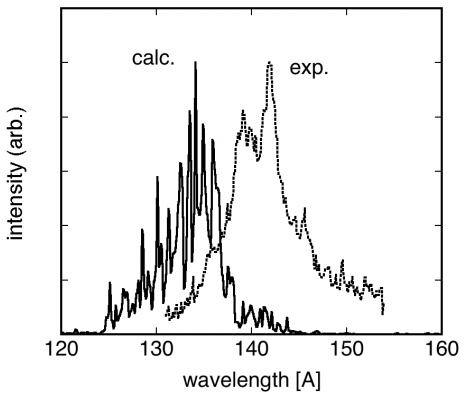

Fig. 4 Comparison between calculated gA value of the $4d - 4f + 4p - 4d$ transition array of Nb-like Sn and emission spectrum observed by charge exchange spectroscopy (CXS) [10].

We note the accuracy of the CR model has been improved by benchmarking of the codes [11]. Comparisons of results obtained from different CR models for the same atomic element, temperature, and density have revealed that a reasonable agreement between codes is obtained by using the same set of atomic levels with sufficient accuracy of the energy of low-lying levels.

3. Structure Formation of Plasmas by the Effect of Radiation Transport

Although the radiative properties of the plasmas can be analyzed using the atomic model, it is sometimes difficult to solve the coupled radiation hydrodynamics to calculate the spatial and temporal profiles of a plasma, especially if the plasma has a non-uniform structure. Such non-uniformity sometimes appears in plasmas for light source applications, which may have an adverse effect on their output characteristics [12].

The opacity of the plasma decreases significantly despite the temperature increase when the number of bound electrons decreases and the outermost shell changes. This behavior can be detected from the fact that as an opaque plasma becomes transparent as ionization proceeds. For instance, in the case of plasmas for EUV sources and x-ray lasers, the emissivity and opacity decreases significantly when the ionization proceeds beyond Ni-like and all bound electrons in $n = 4$ shell are removed. Consequently, the pressure of the plasma, which is determined from the sum of thermal and radiation pressures, changes nonlinearly with respect to the temperature and density.

Such a plasma may show a phase-transition-like behavior. As shown in Fig. 5, if the isotherm on the PV-plane has non-monotonous behavior, structure formation known as spinodal decomposition may occur even in a ther-

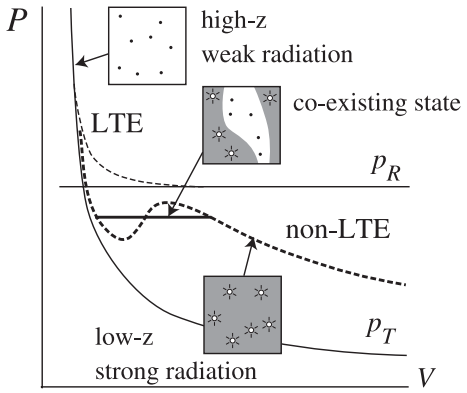

Fig. 5 Schematics of the possible situation to have phase-transition-like behavior in the plasma. Ionization caused by an increase of pressure results in decrease of emissivity and radiative pressure. Total pressure decreases monotonously with the volume in the case of LTE and optically thin condition, however non-monotonous behavior may occur in the non-LTE plasma.

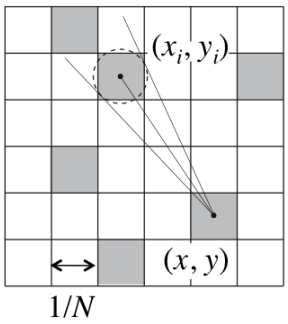

Fig. 6 Schematic diagram for calculation of emission intensity from non-uniform plasmas having co-existence of states of opaque low charged ions and transparent highly-charged ions.

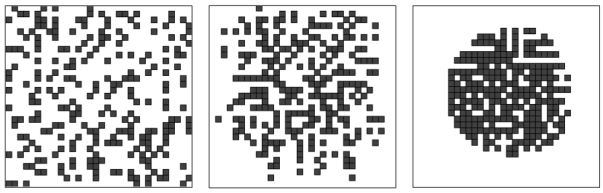

Fig. 7 Example of Monte Carlo calculation of equilibrium state of a plasma. At low temperature, after 10^5 steps, the initial uniform distribution of low-(black) and highly-(white) charged ions becomes circular to minimize the surface area.

mal equilibrium. We consider a simplified atomic model with only two states, an opaque low-charged ions and a transparent high-charged ion states, and their co-existing state is investigated using the Markov chain Monte-Carlo (MCMC) method.

Consider a square with a unit edge length, which is divided by N meshes into cells. Some cells are assumed to be a small "black bodies", which absorb all incoming radiation and emit Planckian radiation from the surface. Other cells are assumed to be transparent. The radiation intensity from the edge can be calculated from the fraction of radiation from each cell; which is not absorbed by any surrounding cells, as shown in Fig. 6.

Given a particular temperature of the system, the most probable state can be obtained by iterative calculations; it is found that at low temperature, the plasma with the low-charged state segregates, because the total intensity from the plasma becomes minimum when the surface area is minimized, as shown in Fig. 7. This suggests that mechanisms similar to surface tension may have caused the structure formation of the plasmas.

4. Summary

In summary, we have shown the present status and possible future plan for the study of atomic processes in plasmas. On the basis of computational atomic data, radiative properties of Sn to Dy plasmas have been investigated. These ions are found to be prospective candidates for the application to EUV sources with wavelengths raging from 62 to 135 nm. For the investigation of low-charged ions with $4f$ open-shell structure, it is suggested that development of a new atomic code along with a method for identification of lines based on a machine learning algorithm may become necessary. As an alternative method for understanding the spatial non-uniformity of the plasmas, the use of the MCMC method to obtain an equilibrium state of the plasma with a simplified atomic and radiative properties is suggested.

Acknowledgement

A part of this study was conducted under the auspices of the Grant-in-Aid for Scientific Research No. 20340166 from the Japan Society for the Promotion of Science (JSPS).

[1] H. Mizoguchi, H. Abe, T. Ishihara, T. Ohta, T. Hori, A. Kurosu, H. Komori, K. Kakizaki and A. Sumitani, Proc. SPIE **7636**, 763608 (2010).
[2] I.V. Fomenkov, A.I. Erashov, W.N. Partlo, D.W. Myers, R.L. Sandstrom, N.R. Böwering, G.O. Vaschenko, O.V. Khodykin, A.N. Bykanov, S.N. Strivastava, I. Ahmad, C. Rajyagur, D.J. Golich, S. De Dea, R.R. Hou, K.M. O'Brien, W.J. Dunstan and D.C. Brandt, Proc. SPIE **7636**, 763639 (2010).
[3] T. Otsuka, D. Kilbane, J. White, T. Higashiguchi, N. Yugami, T. Yatagai, W. Jiang, A. Endo, P. Dunne and G. O'Sullivan, Appl. Phys. Lett. **97**, 111503 (2010).
[4] S.S. Churilov, R.R. Kildiyarova, A.N. Ryabtsev and S.V. Sadovsky, Phys. Scr. **80**, 045303 (2009).
[5] A. Sasaki, A. Sunahara, H. Furukawa, K. Nishihara, S. Fujioka, T. Nishikawa, F. Koike, H. Ohashi and H. Tanuma, J. Appl. Phys. **107**, 113303 (2010).
[6] C.S. Harte, C. Suzuki, T. Kato, H.A. Sakaue, D. Kato, N. Tamura, S. Sudo, R. D'Arcy, E. Sokell, J. White and G. O'Sullivan, J. Phys. B **43**, 205004 (2010).
[7] A. Bar-Shalom, M. Klapisch and J. Oreg, J. Quant. Spectrosc. Radiat. Transf. **71**, 169 (2001).
[8] A. Sasaki, K. Nishihara, A. Sunahara, H. Furukawa, T. Nishikawa and F. Koike, Appl. Phys. Lett. **97**, 231501 (2010).
[9] K. Nishihara, A. Sunahara, A. Sasaki, M. Nunami, H. Tanuma, S. Fujioka, Y. Shimada, K. Fujima, H. Furukawa, T. Kato, F. Koike, R. More, M. Murakami, T. Nishikawa, V. Zhakhovskii, K. Gamata, A. Takata, H. Ueda, H. Nishimura, Y. Izawa, N. Miyanaga and K. Mima, Phys. Plasmas **15**, 056708 (2008).
[10] H. Ohashi, S. Suda, H. Tanuma, S. Fuioka, H. Nishimura, A. Sasaki and K. Nishihara, J. Phys. B **43**, 065204 (2010).
[11] J.G. Rubiano, R. Florido, C. Bowen, R.W. Lee and Y. Ralchenko, HEDP **3**, 225 (2007).
[12] M. Tanaka and T. Kawachi, J. Plasma Fusion Res. **79**, 386 (2003).